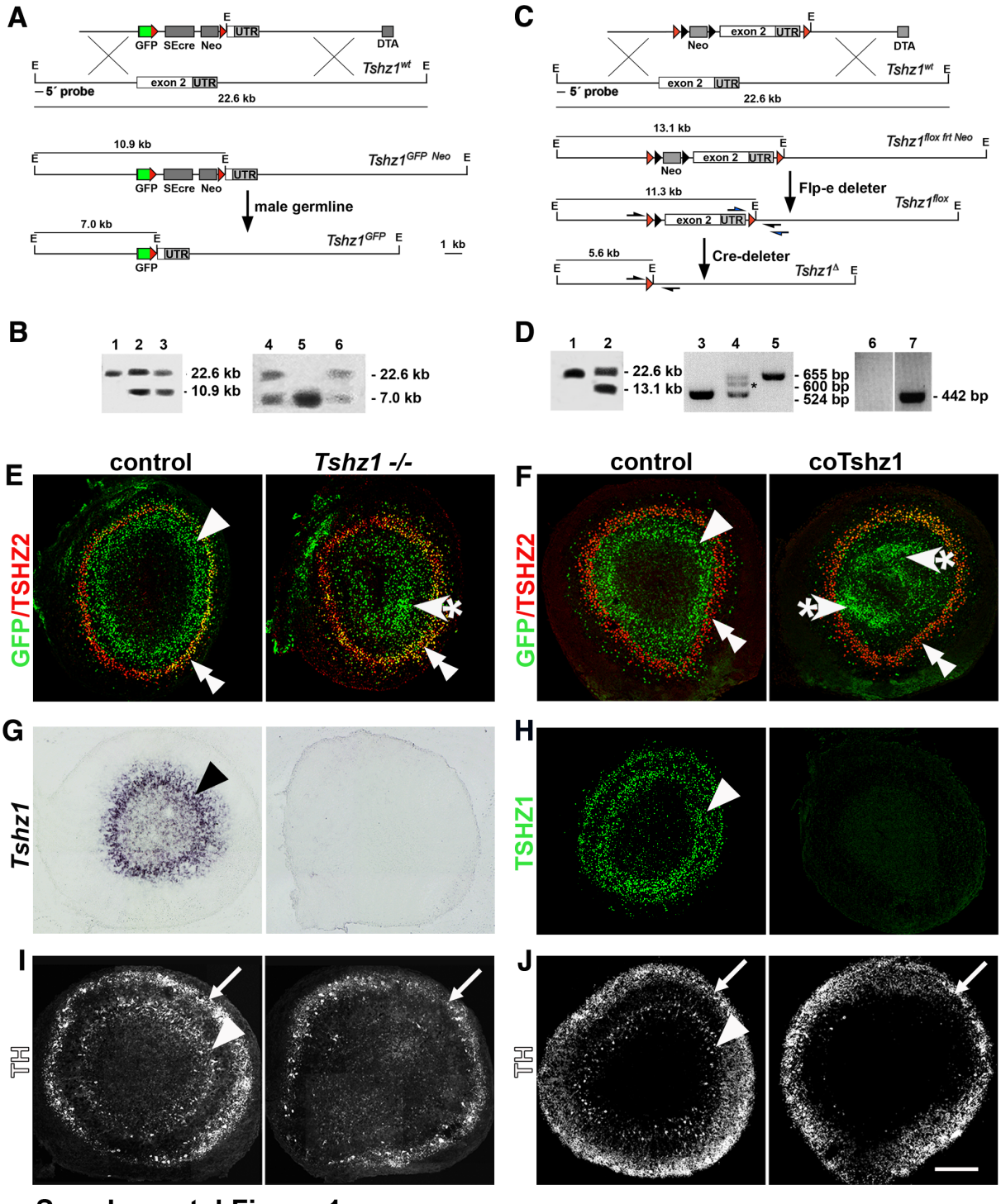

Supplemental Figure 1

Supplemental Figure 1

Gene targeting of *Tshz1* by classical and conditional mutagenesis and *Tshz1* expression in the developing OB in *Tshz1* mutants. (**A**) The targeting vector strategy to generate the $Tshz1^{GFP}$ allele is shown. The GFP cassette (green box), a self-excision cre-neomycin cassette (SEcre Neo) for removal in the male germline, and a diphtheria toxin (DTA) cassette for negative selection are shown. The 3´ end of the *Tshz1* coding sequences (white box), the 3´-UTR of exon 2 (UTR) and *lox*P sites (red arrowheads) are indicated. The sizes of EcoRI restriction enzyme fragments recognized by a probe 5´ of the targeting vector are also indicated. (**B**) Southern blot analysis of EcoRI-digested genomic DNA from ES cells (left panel, lane 1, wild type; lanes 2,3, heterozygote colonies) and newborn mice (right panel, lanes 4,6, heterozygote; lane 5, homozygote mutant) using the 5´ probe. (**C**) The targeting vector used to generate the conditional $Tshz1^{flox}$ allele is shown at the top. *lox*P and *frt* sites are shown as red and black arrowheads, respectively. The neo-cassette was removed after crossing chimeric mice with animals carrying the Flp-e deleter allele. Germline deletion using a cre-deleter strain was used to generate the $Tshz1^{\Delta}$ allele. (**D**) Southern blot analysis of EcoRI-digested genomic DNA from ES cells (left panel, lane 1, wildtype; lane 2, heterozygous colony) and PCR analysis of mice (center panel, lanes 3-5, homozygous wild type, heterozygous $Tshz1^{flox}$/+ and homozygous $Tshz1^{flox/flox}$ mutant, respectively, using primers indicated in blue in (**C**), asterisk indicates a heteroduplex formed by annealing of wild type and mutant DNA strands; right panel, lane 6, heterozygous $Tshz1^{flox}$/+ and lane 7, heterozygous $Tshz1^{\Delta}$/+ mutant, using primers indicated in black in C. Coronal sections of E18.5 OBs were examined by immunohistology (**E**,**F**,**H**-**J**) or in situ hybridization (**G**). The detection of Tshz1 expression by anti-GFP antibodies (green) in control mice revealed a ring of expression in the outer granule cell layer (**E**-**J** arrowheads) directly abutting the $TSHZ2^{+}$ mitral cell layer (**E**,**F**, red, double

arrowheads), and in scattered cells throughout the RMS/subventricular zone of the OB. The staining against the GFP reporter, with a phenotype identical in homozygous *Tshz1*$^{GFP/\Delta}$ (**E**) and coTshz1 (**F**) mutant mice, revealed scattered GFP^{+} cells as well as GFP^{+} aggregates (arrowheads marked by asterisks) located mainly within the inner granule cell layer/subventricular zone of the bulb. (**E**,**F**) Co-expression of the GFP reporter was visible in some of the TSHZ2^{+} mitral cells in control and mutant mice; the organization of the mitral cell layer appeared however unaffected in mutant animals at E18.5. (**G**) Detection of *Tshz1* mRNA in control and *Tshz1* homozygous mutants. (**H**) Staining for TSHZ1 protein (green) in control and coTshz1 mutant animals. (**I**,**J**) Immunostaining of OBs with antibodies directed against tyrosine hydroxylase revealed a loss of this marker in the granule cell layer of mutant mice (arrowheads) while its expression in the glomerular layer was unchanged (arrows). Scale bar: 200 μm (**E**-**J**).

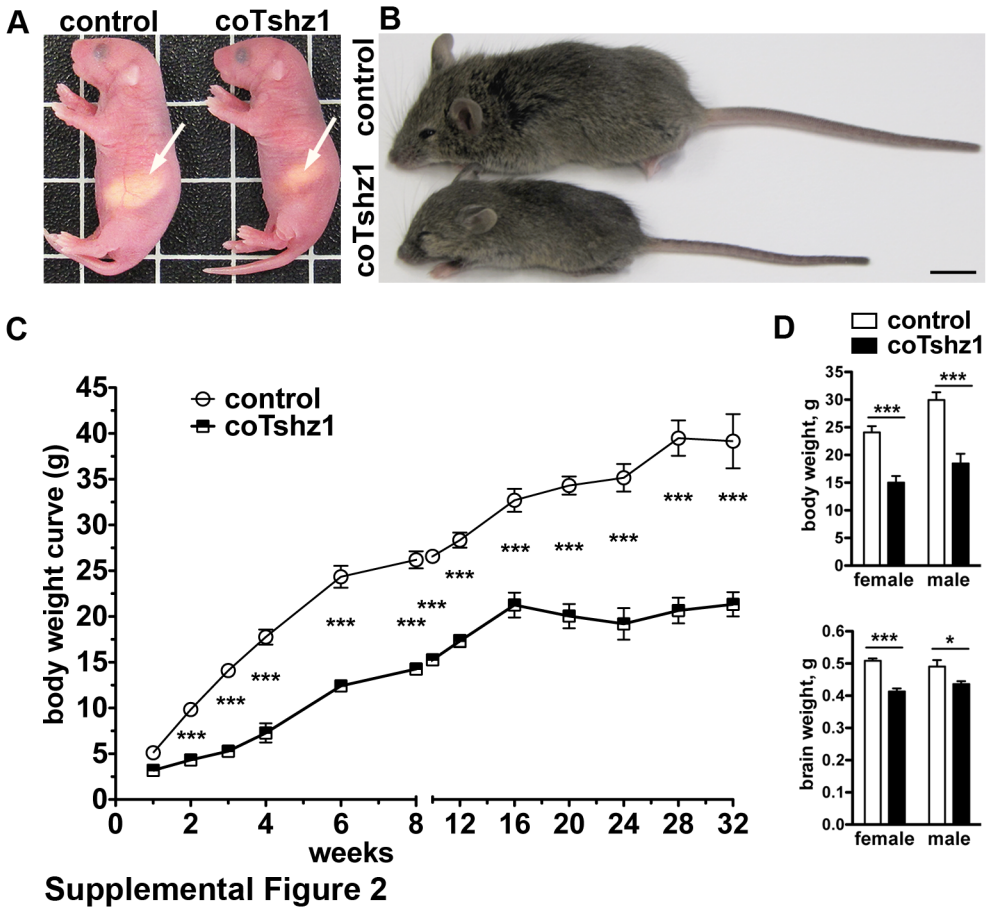

Supplemental Figure 2

Supplemental Figure 2

Phenotypic characterization of coTshz1 mice. (**A**) At P0.5, both control and coTshz1 mutants had suckled, as indicated by the presence of milk in the stomach (arrows). (**B**) Control (upper) and coTshz1 mutant animal (lower) at P21. (**C**) Body weight in control and coTshz1 mutant mice over time. (**D**) Body weight and brain weight (upper and lower panels, respectively) in cohorts of male and female control and coTshz1 mutant mice at 12 weeks of age. Scale bar: 1 cm. **P*< 0.05, ****P*< 0.001.

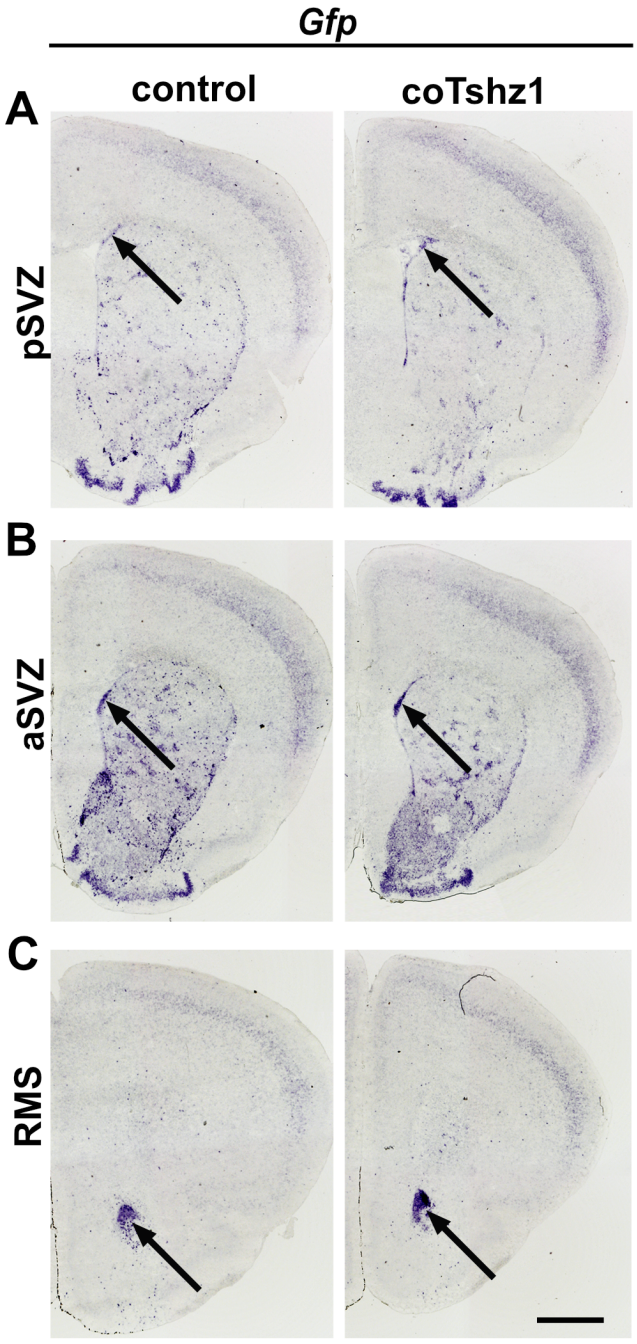

Supplemental Figure 3

Analysis of neuroblasts in the RMS along their route from the lateral ventricle towards the OB in postnatal control and coTshz1 mutant mice. (**A**-**C**) Coronal sections of brains were analyzed by

in situ hybridization with probes against *Gfp*. The morphology of the SVZ/RMS (arrows) prior to entering the OB appeared unaffected in coTshz1 mutant mice. aSVZ, pSVZ, refer to anterior and posterior regions of the subventricular zone, respectively. Scale bar: 1 mm.

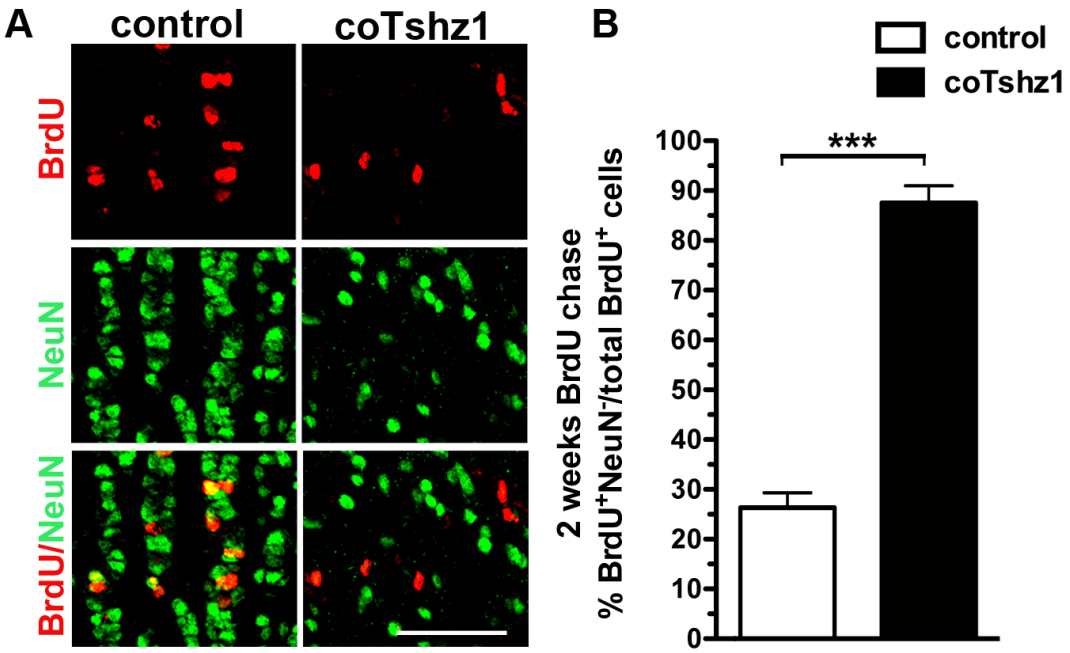

Supplemental Figure 4

Supplemental Figure 4

Differentiation of postnatally born granule cell layer neurons is disrupted in coTshz1 mutants. (**A**) Following a BrdU pulse with a subsequent chase of two weeks, coronal sections of OBs were analyzed by immunostaining for NeuN (green) and BrdU (red). Shown are close-ups of the $NeuN^+$ granule cell layer of controls (left panels) and coTshz1 mutants (right panels). (**B**) The fraction of $BrdU^+NeuN^-$ cells (i.e. those cells that had not yet differentiated into neurons) was determined as a percentage of the total $BrdU^+$ population. Scale bar: 50 μm. ***$P< 0.001$.

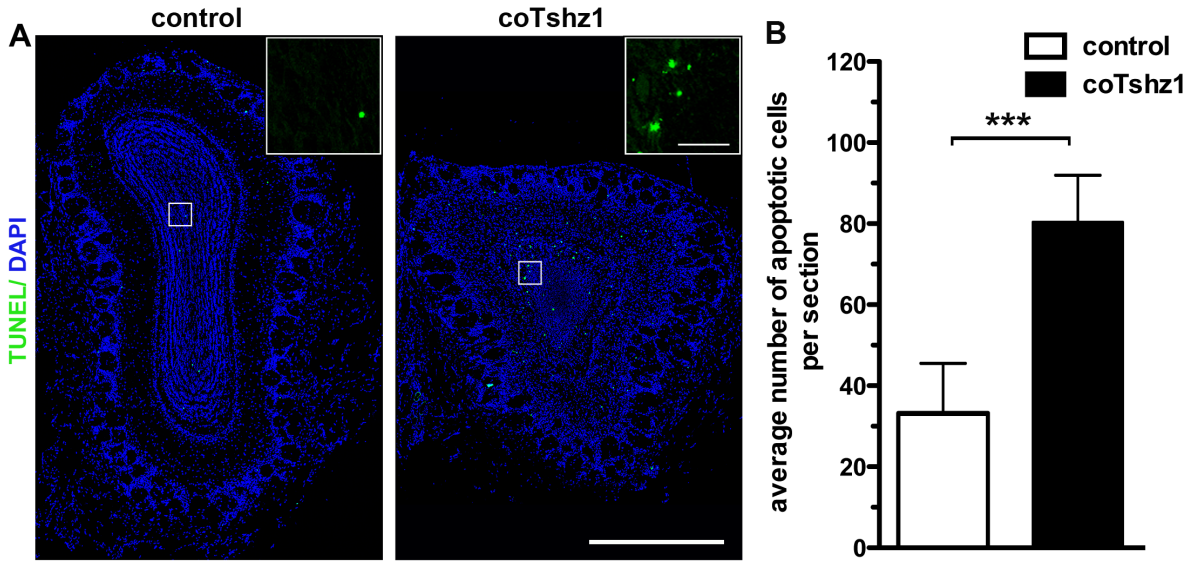

Supplemental Figure 5

Supplemental Figure 5

Increased cell death in the OB of coTshz1 mutant mice. (**A**) Representative pictures show TUNEL-stained apoptotic cells (green) in coronal sections of control and coTshz1 mice. (**B**) Quantification of average number of apoptotic cells per section. Scale bars: 500 μm (**A**), 50 μm (insets). ***$P<$ 0.001.

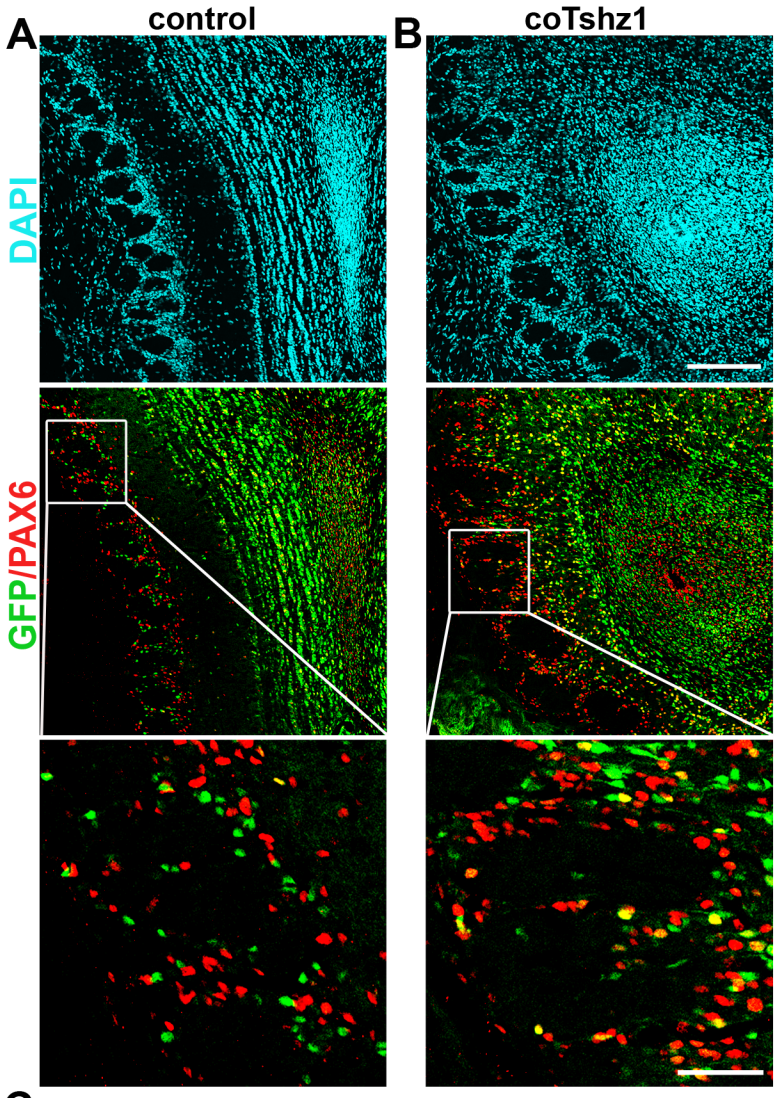

Supplemental Figure 6

Supplemental Figure 6

Immunohistological analysis of coronal sections of the OB in control (**A**) or coTshz1 mutants (**B**) stained with antibodies against GFP (green) or PAX6 (red), and counterstained with DAPI (cyan). Within the glomerular layer of control mice, expression of the GFP reporter and PAX6 was seen in non-overlapping populations of periglomerular neurons (**A**). In coTshz1 mutants, the number of GFP^+ cells around glomeruli was reduced, with many clustering on the inner side of the glomeruli apposing the external plexiform layer (**B**, quantified in **C**). Furthermore, some of these GFP^+ cells also expressed PAX6, implying that *Tshz1* may act to antagonize *Pax6* expression in subsets of periglomerular neurons. Scale bars: 200 μm (A-B), 50 μm (insets). ***$P < 0.001$.

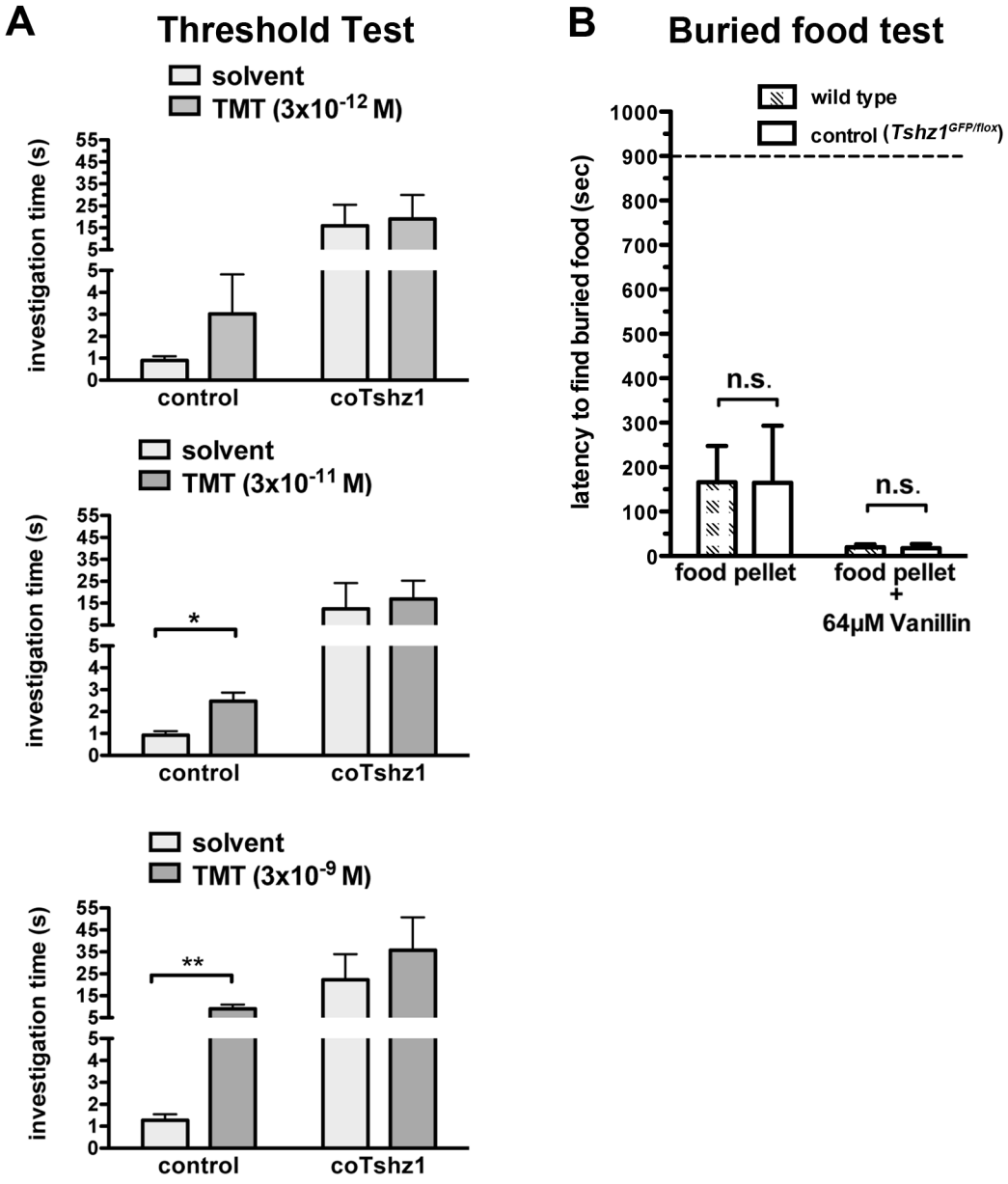

Supplemental Figure 7

Supplemental Figure 7

Behavioral testing of olfaction in control, coTshz1 mutant and heterozygous *Tshz1*^{flox}/- mice. (**A**) The response of animals to a single presentation of the odor TMT on a filter paper at the

concentration indicated, following three presentations of a filter soaked with solvent alone, was determined. Note that the threshold for detection of TMT in control animals was 3 x 10^{-11} M, whilst coTshz1 mutants failed to respond to this odor, even when presented at a 100-fold higher concentration. (**B**) Buried food test with and without vanillin (64 μM) compared between wild type and heterozygous *Tshz1*$^{GFP/flox}$ mice. Values indicate mean± SEM, **P*< 0.05, ***P*< 0.01.

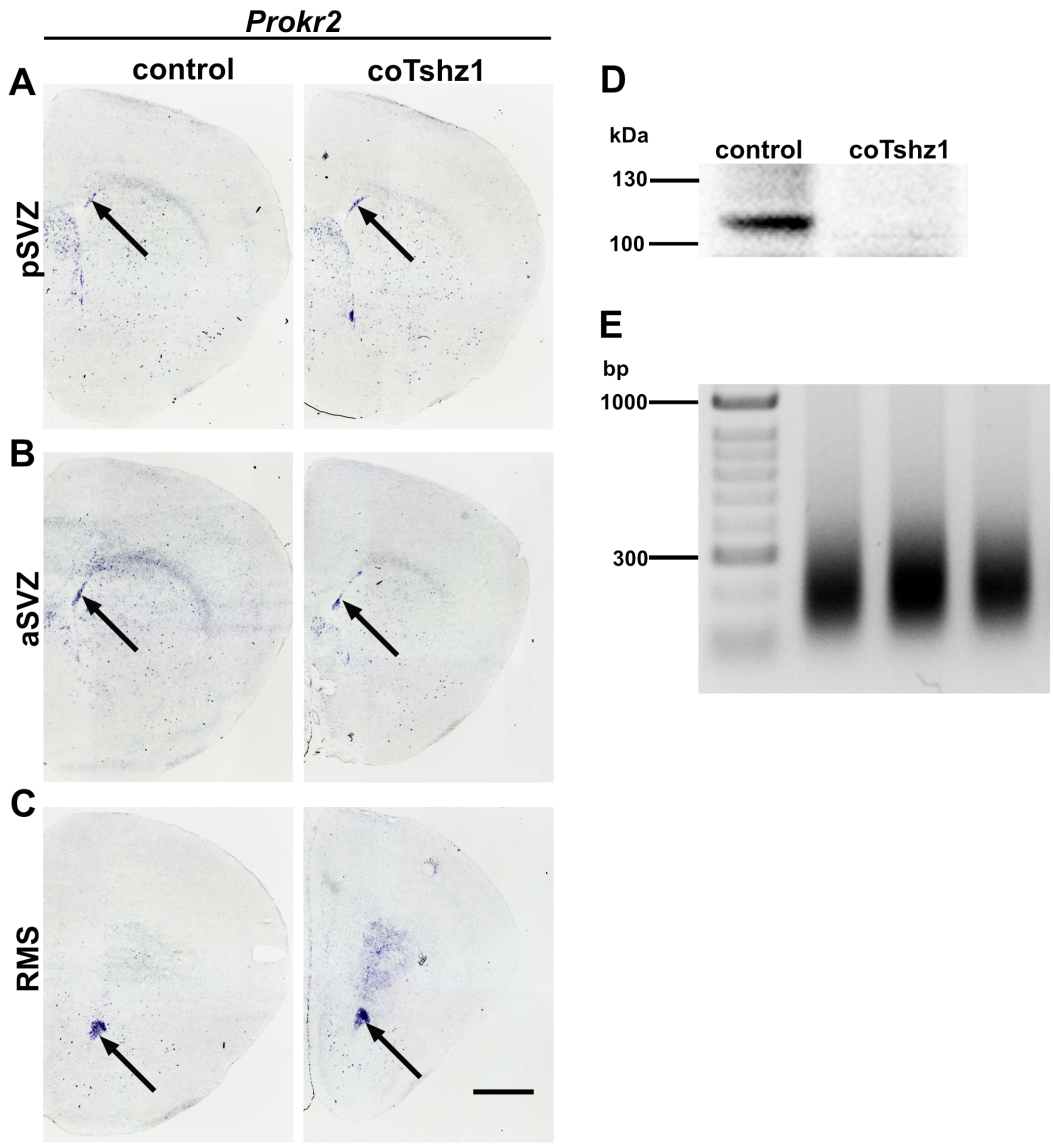

Supplemental Figure 8

Supplemental Figure 8

Expression of Prokr2 in control and coTshz1 mutant adult mice and experimental steps prior to ChIP experiments. (**A-C**) Coronal sections of brains showed no marked changes in *Prokr2* expression in the RMS (arrows) prior to entering the OB in coTshz1 mutant mice. aSVZ, pSVZ, refer to anterior and posterior regions of the subventricular zone, respectively. (**D**) Western blot

analysis with anti-TSHZ1 antiserum that was subsequently used for ChIP experiments detected a protein with the expected size of TSHZ1 (115 kDa) that was present in wild type OB and absent in coTshz1 mutants. (**E**) Sonication of cross-linked DNA from OB tissue for ChIP yielded DNA fragments with sizes up to 1000 bp. Scale bar: 1 mm (**A-C**).

Supplemental Methods

Generation of mice

A 129/SvEvTac mouse BAC clone (RPCI22 library, resource C.H.O.R.I. BACPAC) containing *Tshz1* was identified by Southern hybridization with a *Tshz1* cDNA. A 15 kb DNA fragment containing exon 2 of the *Tshz1* gene was isolated by gap repair (1). Homologous recombination in bacteria was used to generate a targeting vector in which a *GAP43-EGFP* cassette (kindly provided by U. Mueller, The Scripps Research Institute, La Jolla, CA) was fused in-frame following the first five codons of exon 2, while removing most of the open reading frame of *Tshz1* (2.83 kb were deleted) (Supplemental Figure 1A). The encoded fusion protein contains the first 18 amino acids of TSHZ1 (ending in Tyr-Val-Pro-Glu encoded at the start of exon 2), fused to a two amino acid linker preceding the N-terminal 20 amino acids of GAP43, a second two amino acid linker and EGFP sequences, ending with the termination codon of EGFP. The targeting vector also included a self-excision *cre-neo* cassette (2) cloned 3´ of the *GAP43-EGFP* cassette and an MC1-diphtheria toxin A cassette at the 3´-end of the vector for positive and negative selection, respectively. E14.1 ES (129/Ola) cells were electroporated, and colonies that had incorporated the targeting vector into their genome were selected by G418 and analyzed for homologous recombination by Southern blot using 5´ and 3´ sequences situated outside the targeting vector (Supplemental Figure 1B, left panel). C57BL/6 blastocysts were injected with ES cells from heterozygous clones and chimeras mated to C57BL/6 females in order to identify germline transmission (Supplemental Figure 1B, right panel). The $Tshz1^{GFP}$/+ heterozygous strain, in which the self-excision cre-neomycin cassette had been eliminated, was expanded by crossing with C57BL/6 females. Genotypes of offspring were verified by PCR and confirmed by Southern blot hybridization. $Tshz1^{GFP}$/+ mice were viable and fertile, and were used to generate homozygous mutant mice. $Tshz1^{GFP/GFP}$ (*Tshz1*-/-) mutant

animals were born at the expected Mendelian frequency, but contained air in their gastrointestinal tract (aerophagia), failed to suckle, and died within the first day after birth. Similar observations using an independently generated null allele of *Tshz1* have been reported previously (3).

In order to circumvent the embryonic lethality of homozygous *Tshz1* null mutants, we established mice with a $Tshz1^{flox}$ allele. The 15 kb subclone of *Tshz1* (see above) was modified by insertion of a mini targeting vector containing a floxed kanamycin/neomycin resistance cassette (with a dual eukaryotic/prokaryotic promoter) cloned 3´ of the 3´-UTR of the second exon of *Tshz1* (Supplemental Figure 1C). Following expression of cre recombinase in *E.coli*, the resistance cassette was removed, leaving behind a single *lox*P site and an additional EcoRI site. A second mini targeting vector carrying an *frt*-flanked kanamycin/neomycin cassette was inserted 5´ of the second exon. The resulting targeting vector was electroporated into R1 ES cells, the correctly targeted ES cell clones identified by Southern hybridization and injected into C57Bl/6 blastocysts (Supplemental Figure 1D, left panel). Chimeric mice were crossed with Flp-e-deleter female mice (4) to remove the neomycin cassette and the offspring used to establish the $Tshz1^{flox/flox}$ strain (Supplemental Figure 1D, center panel). This was crossed with the germline cre-deleter strain (5) to yield heterozygous animals carrying the $Tshz1^{\Delta}$ allele (Supplemental Figure 1D, right panel), as well as with animals harboring the *nestin-cre* transgene (6) to generate postnatal coTshz1 mutants. Tshz1 expression in controls and coTshz1 mutants ($Tshz1^{GFP/flox}$ and *nes-cre*;$Tshz1^{GFP/flox}$, respectively) was analyzed also by immunohistology and in situ hybridization to verify the cre-dependent ablation of *Tshz1* (Supplemental Figure 1). In contrast to *Tshz1*-/- mutants, which died within the first 24 hours after birth accompanied by severe aerophagia (see above), coTshz1 mutants could suckle and survive during the early postnatal period (Supplemental Figure 2), however a large proportion (approx. 70%) died before analysis during the first four postnatal

weeks. coTshz1 mutants weighed around half that of their littermates (e.g. at P17, control: 9.7 ± 0.5 g, n=19; mutant: 4.7 ± 0.3 g, n=9; $P<0.0001$), and were fed softened food to increase their chances of survival beyond weaning (three to four weeks of age). We used animals of a mix of CD1, 129/Ola, and C57BL/6 for the analysis presented here.

In situ hybridization, histology and immunohistology

Single and double in situ hybridization and immunohistological analyses were performed as previously described (7). For in situ hybridization, brains were freshly embedded into OCT compound and 12 μm frozen sections were cut. Probes for *Tshz1*, Prokineticin 2 (*PK2*), Prokineticin receptor 2 (*Prokr2*), Syntabulin (*Sybu*), Sorting nexin 7 (*Snx7*), G-protein γ-4 subunit (*Gng4*), *Krox20* (*Egr2*), Artemin, *Arc* (activity-regulated cytoskeleton-associated protein), *Dlk1* (delta-like 1), *Notch3*, *Gfap* (glial fibrillary acidic protein), Doublecortin (*Dcx*), Huntingtin associated protein-1 (*Hap1*), c-Kit ligand/Stem cell factor (*Kitl/SCF*), *Gad1* and potassium channel *Kcnj4* were amplified from total brain cDNA, or from genomic DNA in the case of single-exon probes. Probes for calbindin, parvalbumin and calretinin were amplified from cDNA of P15 dorsal root ganglia. Probes for reelin and tyrosine hydroxylase (*TH*) were gifts from Tom Curran, Memphis, USA, and H. Baker, New York, USA, respectively. For immunohistological analysis, adult mice were perfused with 4% paraformaldehyde in 0.1 M sodium phosphate buffer, pH 7.2, tissue was dissected, post-fixed with 4% PFA/phosphate buffer for 2 to 3 hours, cryoprotected in 30% sucrose in PBS, and sectioned at 12 μm. Tissue from embryos and early postnatal mice was dissected, fixed with 4% PFA/phosphate buffer for 2 hours, followed by cryoprotection and sectioning. We employed the following primary antibodies: rat anti-GFP (1:2000, Nacalai Tesque), rabbit anti-PAX6 (1:5000, Chemicon), mouse anti-NeuN (1:500, Chemicon), goat-anti

DCX (1:1000, Santa-Cruz Biotechnology), rabbit anti-GABA (1:5000, Sigma), sheep anti-tyrosine hydroxylase (1:1000, Chemicon), rabbit anti-calretinin (1:3000, Swant), rabbit anti-calbindin (1:3000, Swant) and mouse anti-BrdU (1:200, Sigma). Guinea pig anti-TSHZ1, rabbit anti-TSHZ1 and rabbit anti-TSHZ2 antisera were generated against approximately 100 amino acid fragments (guinea pig and rabbit anti-TSHZ1, codons 592-694; rabbit anti-TSHZ2, codons 551-654), obtained by cloning the corresponding cDNA into pET14b , introducing into BL21 (DE3) pLysS cells and purifying the products with TALLON-Metal-Granulate. Antisera generation was performed by Charles River Laboratories (Sulzfeld). Sections were stained with Cy2-, Cy3- and Cy5-conjugated secondary antibodies (1:500, Jackson Immunoresearch) and counterstained with the nuclear marker DAPI (0.5 µg/ml, Sigma). Fluorescence was imaged on a Zeiss LSM 5 Pascal confocal microscope, and images were processed in Adobe Photoshop. For visualization of the anatomy of the entire RMS in sagittal sections using *Gfp* and *Dcx* in situ hybridization (see Figure 3A,B), micrographs of serial sections were superimposed.

Behavioral tests on mice

The buried food test measures the ability of mice to locate familiar food hidden underneath bedding as described (8). Male and female adult mice (> 12 weeks; n≥ 12 per genotype, food without vanillin, n≥ 4 per genotype, food with 64 μM vanillin) were used. Briefly, naive mice received for three consecutive days in addition to their normal food and water, either cereals alone ("Choco Krispies", Kellogg's) or cereals soaked in an aqueous solution containing 64 μM vanillin (Sigma). Mice were then given access to water on the third night, and the next day were introduced into a clean cage containing a 4 cm-thick layer of bedding, underneath which a single piece of cereal had been hidden. The latency to find this food was recorded in seconds. If the animal failed to find the

food within the 15-minute test period, the animal was placed back into its home cage containing food, and the latency score was set to 900 seconds.

The preference test is designed to identify abilities to sense attractive or aversive odors as described (9, 10) with minor modifications. Male adult mice (>12 weeks; n≥6 per genotype) were used. Briefly, odors, H_2O (neutral), 2-methyl butyric acid (0.9 M, aversive) or peanut butter (10 % w/v aqueous solution, attractive) were introduced to animals in a random order. Each odor (0.5 ml on a 2 cm x 2 cm filter paper) was presented for 3 mins, with an interval of one minute between changes of odor. The total time that the animal spent sniffing at the filter paper within the three-minute test period was recorded in seconds.

The habituation/dishabituation test is designed to determine an animal's ability to habituate to different odors, each of which is presented consecutively three times in a defined order. Mice were exposed three times to one odor, to which they habituated i.e. spent less time sniffing with each consecutive round of presentation. Upon the first presentation of a new odor, the time spent sniffing was typically increased, with habituation being seen during the next two exposures to the same odor. Male adult mice (>12 weeks, n=5 per genotype) were used. Animals were initially exposed to cotton swabs soaked in water, followed by non-social odors (vanilla or cinnamon essence (DM Chemists)) or social odors (male and female urine), each odor being presented three times for three minutes, with one minute intervals between presentations, as previously described (8). The total time spent sniffing in each test period of three minutes was recorded in seconds. For the threshold test, the response of animals to a filter paper soaked with differing concentrations of solvent or odor was determined (10). Animals were exposed three times for three minutes (1 min intervals between presentations) to filter paper (2 cm x 2 cm) containing 20 μl of an aqueous control solution of the organic solvent DEP (Merck), followed by a single presentation of 20 μl of

a solution of the odor TMT (PheroTec, Delta, stock solution dissolved at 0.1% v/v in DEP). The animals were exposed on each day of testing to a single concentration of TMT (3×10^{-12} M, 3×10^{-11} M, or 3×10^{-9} M in ascending order). Data were analyzed by an unpaired t-test to determine significance between the investigation time of the third and fourth trials.

Supplemental References

1. Lee EC, Yu D, Martinez de Velasco J, Tessarollo L, Swing DA, Court DL, Jenkins NA, and Copeland NG. A highly efficient Escherichia coli-based chromosome engineering system adapted for recombinogenic targeting and subcloning of BAC DNA. *Genomics*. 2001;73(1):56-65.
2. Bunting M, Bernstein KE, Greer JM, Capecchi MR, and Thomas KR. Targeting genes for self-excision in the germ line. *Genes Dev*. 1999;13(12):1524-1528.
3. Coré N, Caubit X, Metchat A, Boned A, Djabali M, and Fasano L. Tshz1 is required for axial skeleton, soft palate and middle ear development in mice. *Dev Biol*. 2007;308(2):407-420.
4. Rodriguez CI, Buchholz F, Galloway J, Sequerra R, Kasper J, Ayala R, Stewart AF, and Dymecki SM. High-efficiency deleter mice show that FLPe is an alternative to Cre-loxP. *Nat Genet*. 2000;25(2):139-140.
5. Schwenk F, Baron U, and Rajewsky K. A cre-transgenic mouse strain for the ubiquitous deletion of loxP-flanked gene segments including deletion in germ cells. *Nucleic Acids Res*. 1995;23(24):5080-5081.
6. Tronche F, Kellendonk C, Kretz O, Gass P, Anlag K, Orban PC, Bock R, Klein R, and Schutz G. Disruption of the glucocorticoid receptor gene in the nervous system results in reduced anxiety. *Nat Genet*. 1999;23(1):99-103.
7. Watakabe A, Ichinohe N, Ohsawa S, Hashikawa T, Komatsu Y, Rockland KS, and Yamamori T. Comparative analysis of layer-specific genes in Mammalian neocortex. *Cereb Cortex*. 2007;17(8):1918-1933.
8. Yang M, and Crawley JN. Simple behavioral assessment of mouse olfaction. *Curr Protoc Neurosci*. 2009;48:8.24.1-8.24.12.
9. Witt RM, Galligan MM, Despinoy JR, and Segal R. Olfactory behavioral testing in the adult mouse. *J Vis Exp*. 2009;(23).
10. Kobayakawa K, Kobayakawa R, Matsumoto H, Oka Y, Imai T, Ikawa M, Okabe M, Ikeda T, Itohara S, Kikusui T, et al. Innate versus learned odour processing in the mouse olfactory bulb. *Nature*. 2007;450(7169):503-508.